Research Article ISSN 2771-666X

Journal of Advanced Materials Science and Engineering

Investigation of Zinc Corrosion in Tropical Soil Solution

Lebrini M[1*], Salhi L[2], Deyrat C[3], Roos C[1] and Nait-Rabah O[2]

[1]*Laboratoire Matériaux et Molécules en Milieux Agressif; EA 7526, Campus Universitaire de Schoelcher B.P. 7209 F- 97275 Schoelcher, Martinique, France.*

[2]*EcoFoG-Université de la Guyane, 97351 Cayenne, French Guiana.*

[3]*Guyafor, 97355 Macouria, French Guiana.*

[*]Correspondence:
Lebrini M, Laboratoire Matériaux et Molécules en Milieux Agressif; EA 7526, Campus Universitaire de Schoelcher B.P. 7209 F- 97275 Schoelcher, Martinique, France.

Received: 05 Feb 2023; **Accepted:** 11 Mar 2023; **Published:** 16 Mar 2023

Citation: Lebrini M, Salhi L, Deyrat C, et.al,. Investigation of Zinc Corrosion in Tropical Soil Solution. J Adv Mater Sci Eng. 2023; 3(1): 1-7.

ABSTRACT

The paper presents a large experimental study on the corrosion of zinc in tropical soil and in the ground water at the various depths. Through this study, the corrosion rate prediction was done based on two methods the electrochemical method and the gravimetric. The electrochemical results showed that the corrosion rate is more important at the depth levels 0 m to 0.5 m and 0.5 m to 1 m and beyond these depth levels, the corrosion rate is less important. The electrochemical results indicated also that a passive layer is formed on the zinc surface. The found SEM and EDX micrographs displayed that the surface is extremely attacked and confirmed that a zinc oxide layer is present on the surface whose thickness and relief increase as the contact with soil increases.

Keywords

Soil-Corrosion, Galvanized steel, Electrochemical techniques, SEM and EDX.

Introduction

The structural integrity of metal components suppressed underground is mostly affected by corrosion, which may cause eventually total failure. Soil-corrosion is a multifaceted phenomenon, with many factors are complicated. The main factors are detected to be type of soil, geo technical properties, soil resistivity, pH, sulfate content, chloride content, sulfide ion content etc., [1-4]. Several attempts have been made to study and to predict the extent of corrosion by correlating various soil parameters with observed rates of corrosion [5-10]. Galvanized steel is extensively used in various manufacturing purposes for its resistance to corrosion. This improved corrosion comportment is known by the zinc coating in two steps: firstly, reacting as physical barrier, and then, providing galvanic protection [11].

The purpose of this study is the investigation of zinc corrosion in artificial tropical soil solution and in ground water at the different depths. The presented results are obtained for period of 8 months for surface soil conditions by corrosion testing in the selected site. The corrosion rate was measured under varying soil condition. The mechanism of soil-corrosion was carried out by weight loss and electrochemical measurements. SEM and EDX were used for the surface analysis

Materials and Methods

Investigation Site and Solution

The testing site is located in tropical environmental of French Guiana. The tropical region is characterized by strong sunlight in two seasons (the dry season and rainy season). The soil is characterized by height moisture. Five area were selected to represent medium to dense sandy loam (i.e. cohesionless material). For each area, the recovery of soil samples has been carried out at each depth: 0 m to 0.5m, 0.5 m to1 m, 1 m to 1.5 m, 1.5 m to 2 m and 2 m to 2.5 m. The soil was characterized in two seasons.

Table 1: Chemical Parameter of the Soil Solution In-Situ (Rainy Season).

Depth (m)	*0-0.5*	*0.5-1*	*1-1.5*	*1.5-2*	*2-2.5*
pH	4.14	3.91	3.88	3.57	3.53
CE (µS/cm)	457	404	483	497	498
Cl^- (mg/L)	139	114	139	6	10
SO_4^{2-}(mg/L)	6.3	81	33	21	18
Ca^{2+} (mg/L)	10	17	22	14	5
Mg^{2+}(mg/L)	5.18	6	5	8	9
Na^+ (mg/L)	33	26	30	36	43
K^+ (mg/L)	44	13	10	7	8
Al^{3+} (mg/L)	21	18	13	2	1
Fe^{3+} (mg/L)	9	7	10	0.4	0.2
NO_3^-(mg/L)	1.6	2	1	1	1

The chemical parameters of the soil solution are shown in Tables 1 and 2. Only one area have been represented in the Tables 1 and 2; the other areas give similar values. The relevant standard NF X31-107 was used for the determination of the quantities of minerals [12] and the ISO 10390 for the determination of pH [13]. The colorimetric method was used for the chloride and nephelometric method was used for sulphate contents in aqueous extract [14]. The relevant standard NF T 90-019 was used for Na^+, Ca^{2+}, Mg^{2+}, K^+, $Al3^+$ and Fe^{3+} contents in aqueous extract [15]. The conductivity has been measured in accordance with the standard NF EN 27888 [16], NF ISO 11464 for the soil moisture [17]. Chemical analysis in both seasons shows that the soil is significantly more acidic in the rainy season (pH = 3.7-3.9) than in the dry season (pH = 4.5-5.5). In addition, the soil composition is dissimilar. Indeed, there is an increase in sulphate, aluminum and iron concentrations in the dry season. The chemical analysis was carried out in order to prepare the artificial soil solution for the electrochemical tests. The concentration of each ion in the artificial soil solution has been calculated taking account the real moisture, the conductivity and pH of soil. The composition of the artificial soil solution for each depth is summarized in Table 3.

For all depth ranges, the values of conductivity and pH are quite close to the actual measured average values. This chemical composition makes it possible to show, if necessary, a correlation between the corrosion rate and the concentrations of chemical elements. For the evaluation of the corrosion rate in the studied soil, this composition will be retained because it best represents the chemical profile of the soil with rather small standard deviations.

Table 2: Chemical parameter of the soil solution in-situ (dry season - 8 months of soil-pile contact).

Depth (m)	*0-0.5*	*0.5-1*	*1-1.5*	*1.5-2*	*2-2.5*
pH	5.60	4.95	4.95	4.95	4.34
CE (µS/cm)	462	310	352	240	228
Cl^- (mg/L)	27	21	26	28	32
SO_4^{2-}(mg/L)	214	250	700	50	141
Ca^{2+} (mg/L)	4	1	0.4	0.6	0.4
Mg^{2+}(mg/L)	13	12	8	0.6	1
Na^+ (mg/L)	53	25	39	31	24
K^+ (mg/L)	37	13	7	6	6
Al^{3+} (mg/L)	130	220	260	13	7
Fe^{3+} (mg/L)	186	330	650	27	16
NO_3^-(mg/L)	1.6	1.5	0.9	1	0.9

Table 3: The Artificial soil solution.

Depth (m)	*0-0.5*	*0.5-1*	*1-1.5*	*1.5-2*	*2-2.5*
pH	3.79	3.76	3.82	3.83	3.83
CE (µS/cm)	402	347	327	299	298
Cl^- (mg/L)	77	68	65	57	54
SO_4^{2-}(mg/L)	[24]	19	17	15	17
Ca^{2+} (mg/L)	7	6	6	6	4.5
Mg^{2+}(mg/L)	3.6	3.5	3.5	3.5	3.5
Na^+ (mg/L)	30	25	22	22	22
K^+ (mg/L)	15	9	8	6	6
Al^{3+} (mg/L)	15	10	11	5	5
Fe^{3+} (mg/L)	10	11	9	9	9

The Electrochemical Tests

The experiments were carried out using a standard electrochemical three-electrode cell. The corrosion tests have been carried out on electrodes cut from sheets of zinc. The reference electrode was a saturated calomel electrode. All the reported potential values are referred to this type of electrode. Before each Tafel and EIS experiments, the electrode was allowed to corrode freely and its open circuit potential (OCP) was recorded as a function of time during 3 hours, the time necessary to reach a quasi-stationary value for the open-circuit potential. This steady-state OCP corresponds to the corrosion potential (E_{corr}) of the working electrode. The anodic and cathodic polarisation curves were recorded by a constant sweep rate of 20 mV/min. Electrochemical impedance spectroscopy (EIS) measurements were carried out, using ac signals of amplitude 5 mV peak to peak at different conditions in the frequency range of 100 kHz to 10 mHz.

Electrochemical measurements were performed through a VSP electrochemical measurement system (Bio-Logic). The above procedures were repeated two times with success for each test. The Tafel, R_p fit and EIS data were analyzed and fitted using graphing and analyzing impedance software, version EC-Lab V9.97.

Weight Loss Measurements

The gravimetric method has been used to evaluate also the corrosion rate of zinc in soil of tested site. Therefore, 14 coupons of zinc are considered in this study. Then all coupons were embedded in soil of tested site at depth 0.5 m. This depth has been selected because the soil has the highest conductivity and the more acidic (CE=517 µS/cm and pH=3.7) and the corrosion rate is more important. The exact dimensions of each coupon were measured using a caliper. Before the embedding in soil, each set of coupons (1mm) was thoroughly polished with a SIC paper of 1200, washed with distilled water and acetone to remove any residual oils. The coupons were dried and each coupon was weighted on an analytical balance.

Surface Analysis

The surface morphology was imaged using an environmental scanning electron microscope (ESEM–F.E.I Quanta 250). Before surface analysis, the zinc disk was rinsed with ethanol and dried in air at room temperature. The EDX was done to present general composition of the surface. The measurements were performed using an EDAX GENESIS APEX 2i with SDD Detector (Silicon

Drift Detector) without nitrogen liquid makes it possible to perform EDX spectra and therefore to perform chemical analyzes qualitative and quantitative.

Results and Discussion

Electrochemical Results

Figures 3 and 4 display the Nyquist plots for zinc in the artificial soil solution at different depth level. The impedance diagrams obtained show the same trend for the depth 0 m to 0.5 m and 0.5 m to 1 m; one capacitive loop, which related to the charge-transfer resistance. The impedance diagrams revealed two depressed capacitive semicircles for the depth 1m to 1.5m and 2 m to 2.5 m. The primary loop, in height frequencies, is related to the charge transfer, though the second capacitive loop is attributed to the passive layer due to the products of corrosion [18].

The impedance diagrams display an important electrolyte resistance for all the depth range. The important electrolyte resistance is due to the presence of various cations in the solution, which increase the electrolyte resistance.

The obtained data were fitted by the corresponding circuit given in Figures 3 and 4. Each equivalent circuit is adjusted to the corresponding system with one or two phenomena. According to the fit, the zinc electrode had the parameters of R_t = 1.3 kΩ.cm^2 and 1.4 kΩ.cm^2 for the depth 0 m to 0.5 m and 0.5 m to 1 m, respectively. When the system represented by two capacities, the zinc electrode had the parameters R_t = 425 Ω.cm^2 and 500 Ω.cm^2 for the charge-transfer resistance and R_{pc} = 1 kΩ.cm^2 and 1.25 kΩ.cm^2 for the passive layer for the depth 1m-1.5m and 2m-2.5m, respectively.

Polarisation curves for zinc in the artificial soil solution at different depth level are shown in Figure 2. This Fig. shows that the anodic slope is similar for different depth level. It is noted that the cathodic region was more affected than the anodic region. The depths 1.5 m to 2 m and 2 m to 2.5 m display a different behavior, where we note a peak towards -1200 mV on the cathodic regions of the curves. Witch can be associated to the presence of a passive layer. A passivation of zinc by the formation of $Zn_5(OH)_8Cl_2{\cdot}2H_2O$ was noted. The presence of the peak at -1224mV is attributed to the reduction of corrosion product [19-21]. It should be noted that the corrosion potential values do not vary and has not been changed significantly with respect to depth; Figure 1. The polarization confirms the two different electrochemical behavior observed by impedance results.

Values of associated electrochemical parameters are presented in Table 4. The calculated corrosion rate of the zinc from the corrosion current (I_{corr}) according to "(1)" [20-23] is also given in the Table 4.

$$V_{corr}\ (mm.year^{-1}) = 0.00327 * M * I_{corr}/n * d) \quad (1)$$

Where M is the atomic mass of zinc (g/mol), n is the number of electrons exchanged in the corrosion reaction and d is zinc density (g/cm^3).

The polarization results indicated that the I_{corr} values decreased and Rp values increased with respect to depth level.

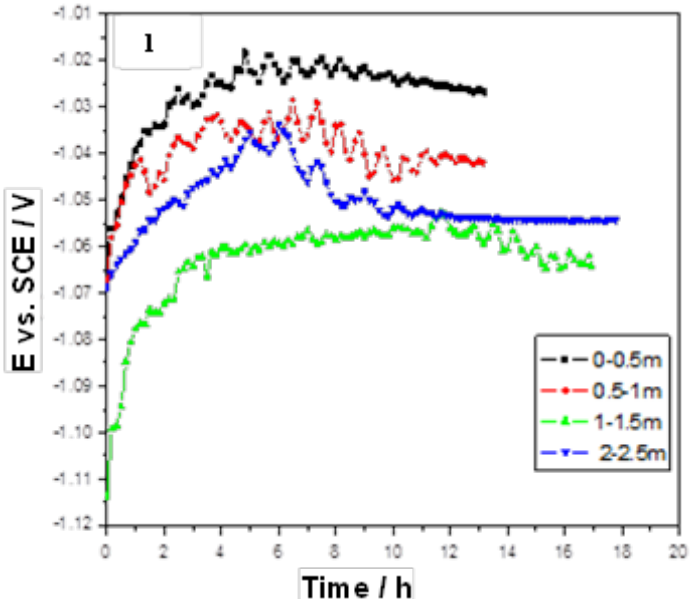

Figure 1: Variation of the open-circuit potential of zinc corrosion in the artificial soil solution.

No specific tendency was seen in the shift of E_{corr} values and depth; however, we could note that the corrosion rate decreases with increase in depths. The corrosion rate is more important at the depth levels 0 m to 0.5 m and 0.5 m to 1 m. This strong corrosion is due to the high concentration of Cl^- and SO_4^{2-} ions and is due to the important conductivity at these levels. Beyond these depth levels, the corrosion rate is less important. Because the ions concentration and the conductivity are low, and on the other hand, at these depths the presence of a passive layer decreases the corrosion.

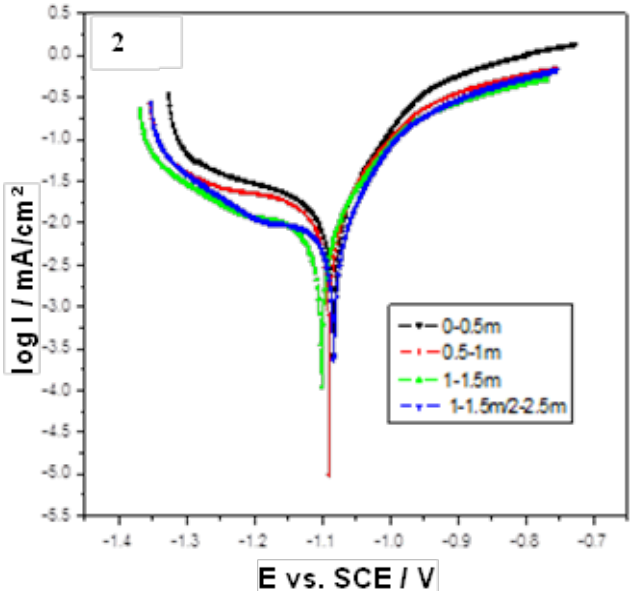

Figure 2: Polarization curves of zinc corrosion in the artificial soil solution.

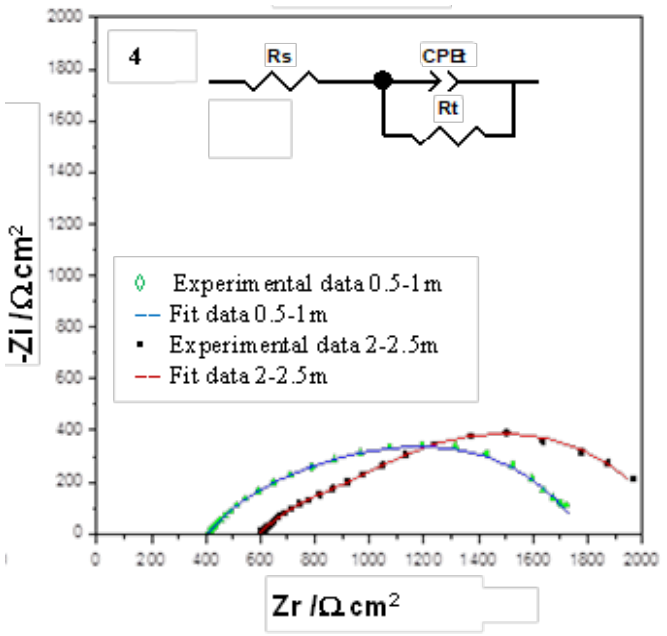

Figure 3: Nyquist plots and Equivalent circuit used to fit impedance data of zinc corrosion in the artificial soil solution at the depth levels 0.5 m to 1 m and 2 m to 2.5 m.

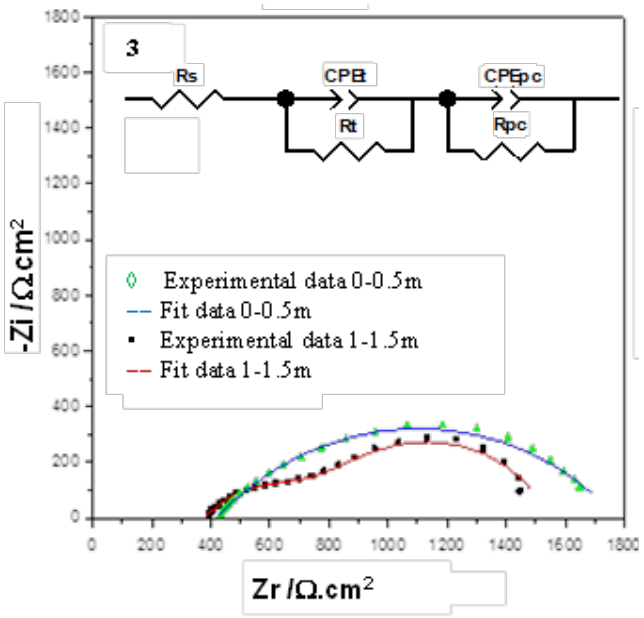

Figure 4: Nyquist plots and Equivalent circuit used to fit impedance data of zinc corrosion in the artificial soil solution at the depth levels 0 m to 0.5 m and 1 m to 1.5 m.

Table 4: Electrochemical Parameters Obtained From Polarisation Curves.

Depth (m)	*0-0.5*	*0.5-1*	*1-1.5*	*1.5-2*	*2-2.5*
pH	3.8	3.7	3.8	3.8	3.8
***CE* µS/cm**	402	347	327	299	298
I_{corr} **µA/cm²**	13	12	10	8	8
R_p **Ω/cm⁻²**	1665	2000	2235	2595	3030
E_{corr} **mVvsSCE**	-1085	-1091	-1102	-1093	-1093
V_{corr} **mm/year**	0.200	0.179	0.149	0.124	0.124

Gravimetric Results

As reported in the electrochemical results section, the 0 m to 0.5 m depth showed the most significant corrosion due to the acidic pH and an important conductivity. It seemed more judicious to carry out the weight loss tests only at the 0 m to 0.5 m depth. The values of weight loss and corrosion rate for different immersion periods are shown in Figure 4. The weight loss corresponds to a contact time *t*, is given by using the following expression:

$$\Delta w(mg) = w_0 - w_t \quad (2)$$

The corrosion rate (V_{corr}) expressed with mg.cm^{-2}.h^{-1} of the zinc was calculated from the weight loss (Δw) using the following expression:

$$V_{corr}\ (mg.cm^{-2}.h^{-1}) = \Delta w/(S * t) \quad (3)$$

Or with mm/year:

$$V_{corr}\ (mm.year^{-1}) = 87.6\Delta w/d * S * t) \quad (4)$$

Where: *t* is the exposure period (*h*), *d* is the density of the metal (g/cm^3) and *S* is the surface area of the metal coupon (cm^2).

It's found that the weight loss decreases with increase in immersion time and remains stable from 115 days. The coupons were buried during the rainy season. Or, the corrosion rate is greater in this season. Decreased corrosion rate may be due to decreased in soil moisture in the dry season. Since the phreatic layer is below the depth where they were positioned our samples.

SEM and EDX micrographs obtained from zinc surface at different immersion periods are show in Figure 6. This figure reveals that the surface is highly corroded and shows that a layer of zinc oxide is present on the surface whose thickness and relief increase as the contact with soil increases. The presence of the oxide zinc layer can explain the decrease of the corrosion rate by the formation of a protective layer on the surface.

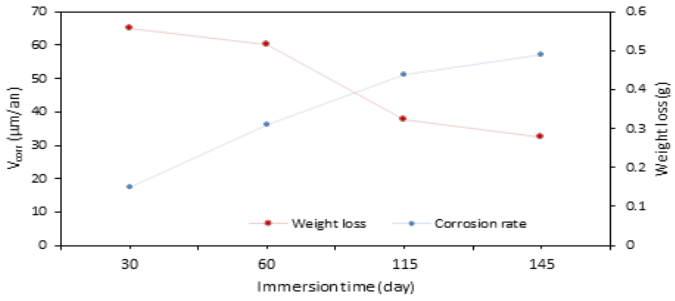

Figure 5: Corrosion rate and weight loss of zinc after different immersion periods at the depths 0 m to 0.5 m.

Investigation of Zinc Corrosion after 8 Months of Soil-Contact

The investigation of zinc corrosion after 8 months of soil-contact was too considered, the obtained electrochemical results are shown in Figures. 7 and 8. The polarization curves indicate a clear shift in the cathodic parts and a less extent in the anodic parts. Moreover,

the values of corrosion potential E_{corr} for all the depths varies from -1.10 to -1.02 V after 14 hours of immersion. The peak around 1.2 V, characteristic of the passivation layer is still present. It is more remarkable for depths beyond 1.5m. The Nyquist diagrams; display a different electrochemical behavior after 8 months of soil-contact unlike the one before. This behavior is characterized by the presence of two capacitive loops for all depth ranges, illustrated in Figure 8 (representative example). The electrochemical results obtained from polarization curves and the values of conductivity and pH for all depth ranges are reported in Table 5. The calculated corrosion rate is correlated to the conductivity and pH.

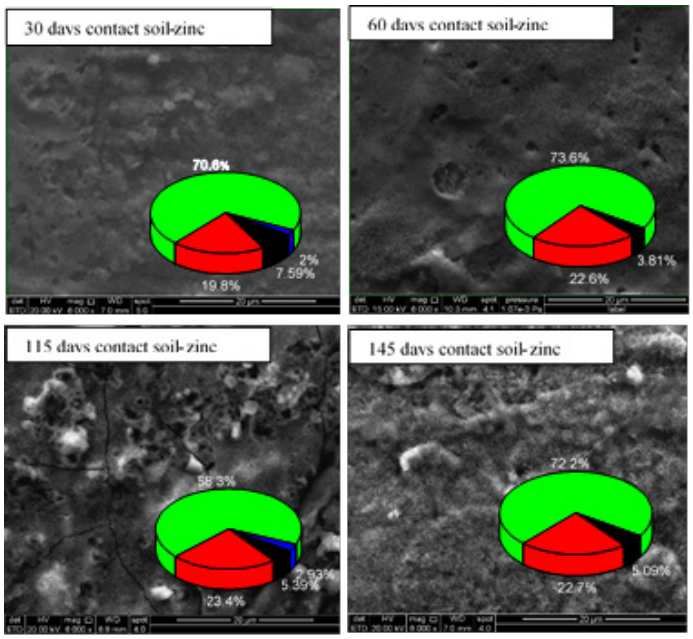

Figure 6: SEM micrographs of zinc at different immersion periods at the depths 0 m to 0.5 m.

The obtained results reveal that the I_{corr} values remains considerably unchanged and a further increase in depth did not make any variation in the corrosion rate. It is also noted that, although the pH is minimal for depth 2 m to 2.5 m, the corrosion rate is the lowest in this area. It is also noted that the corrosion rate does not seem to be related to the conductivity obviously. The found results were in accordance with the study conducted by Roseana et al. [24] where they showed that the corrosion rates observed did not reflect the aggressiveness degree indicated through specific index based on resistivity and other parameters.

Figure 9 shows SEM and EDX micrographs for the different electrodes used corresponding to each depth level. The electron micrographs are different and show the presence of oxide and hydroxide (probably iron) on the surface of the electrodes in the 0.5 m to 1.5 m depth range. The mass percentage of iron between 0.5 m and 1 m and between 1 m and 1.5 m is respectively 25 and 40%. Iron content in solution is important for depths 0.5 m to 1 m and 1 m to 1.5 m. It is possible that at a pH=5, a precipitation of the iron hydroxide was done and that it was deposited on the electrode. No trace of iron was found beyond 1.5 m. The presence of aluminum is difficult to explain, especially since at these depths its concentration is low.

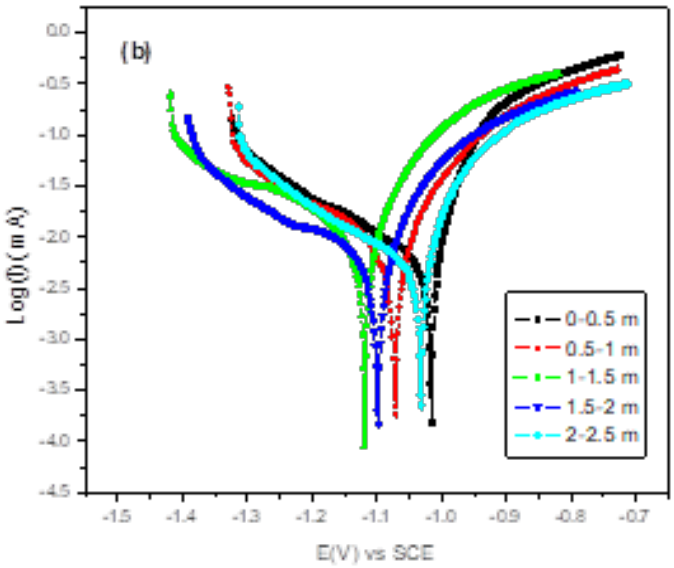

Figure 7: Polarization curves for zinc at different depth level.

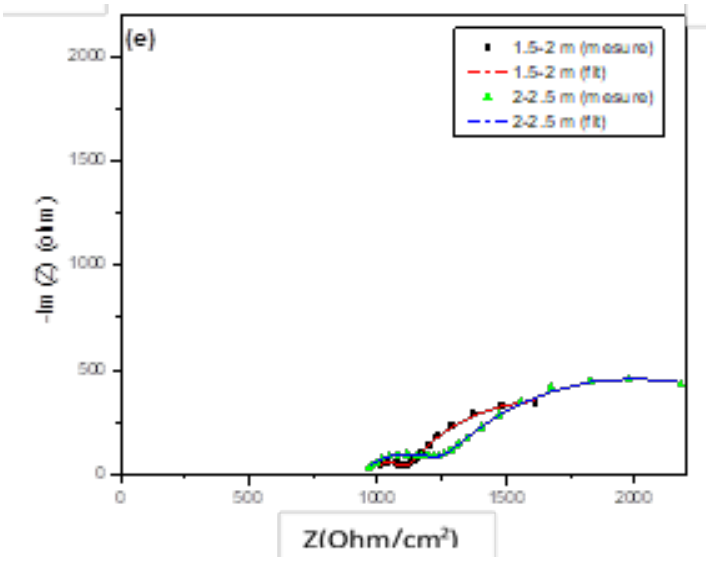

Figure 8: Nyquist plots for zinc at depth 1.5 m to 2 m and 2 m to 2.5 m.

Conclusion

The investigation of Zinc Corrosion in artificial tropical soil solution revealed the following results:

- The impedance results indicated two different electrochemical behavior described by one capacitive loop for the depth 0 m to 0.5 m and 0.5 m to 1 m and two depressed capacitive semicircles for the depth 1m-1.5 and 2 m to 2.5 m.
- The polarisation noted that the cathodic part was more affected than the anodic region and noted also the presence of a peak towards -1200 mV, which can be associated to the presence of a passive layer.

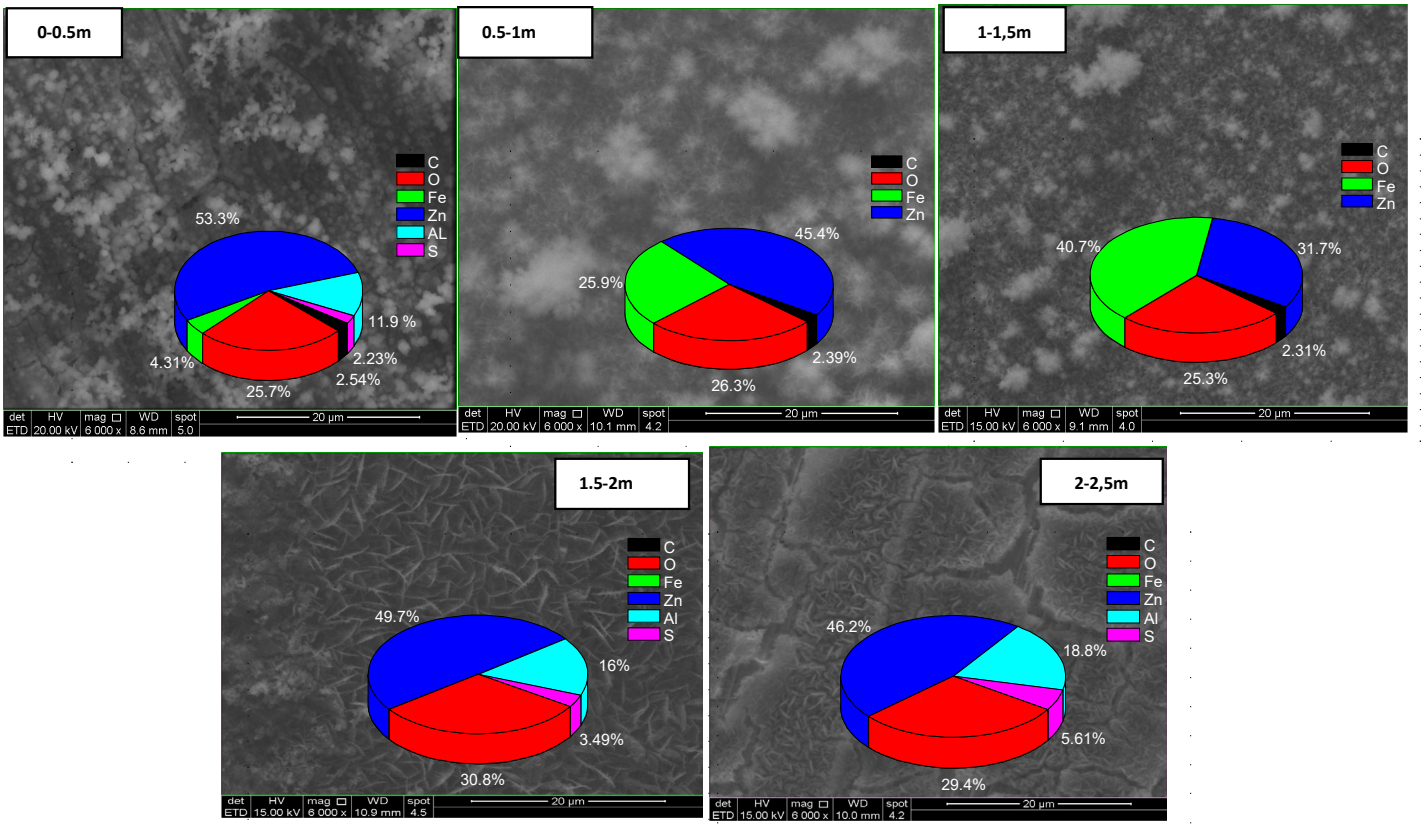

Figure 9: SEM and EDX micrographs for the different electrodes at each depth level.

- The electrochemical methods showed that the corrosion rate is more important at the depth levels 0 m to 0.5 m and 0.5 m to 1 m and beyond these depth levels, the corrosion rate is less important.
- The gravimetric method indicates that the weight loss decreases with increase in immersion time and remains stable from 115 days. SEM and EDX micrographs show the presence of the oxide zinc layer on the surface.

Acknowledgement

This work was supported by European Union through PROMES framework (European Development Funds, program: No.31567) and the PhD grant by ANRT-Agency (CIFRE No 975/2011).

References

1. Peabody AW. Control of Pipeline Corrosion: Second ed. NACE Press, Houston. 2001; 211-236.
2. Chaker V, Palmer JD. ASTM Committee G-1 on Corrosion of Metals. Effect of Soil Characteristics on Corrosion. ASTM Inter. 1989; 81.
3. Noor NM, Yahaya N, Othman SR, et al. New Technique for Studying Soil-Corrosion of Underground Pipeline. J. Appl. Sci. 2011; 11: 1510-1518.
4. Ikechukwu AS, Obioma E, Ugochukwu NH. Studies on corrosion characteristics of carbon steel exposed to Na2CO3, Na2SO4 and NaCl solutions of different concentrations. Int. J. Eng. Sci. 2014; 3: 48-60.
5. Suganya S, Jeyalakshmi R, Rajamanec NP. Corrosion behavior of mild steel in an in-situ and ex- situ soil. Mater. Today: Proc. 2018; 5: 8735-8743.
6. Seolin S, Gunhak L, Usama A, et al. Risk-based underground pipeline safety management considering corrosion effect. J. Hazard. Mater. 2018; 342: 279-289.
7. Galai M, choucria J, Hassani Y, et al. Moisture content and chloride ion effect on the corrosion behavior of fitting brass (gate valves) used as a connection of PVC's conduits in aggressive sandy soil. Chem. Data Collect. 2019; 19: 100171.
8. Karthick S, Muralidharan S, Saraswathy V. Corrosion performance of mild steel and galvanized iron in clay soil environment. Arab. J. Chem. 2020; 13: 3301-3318.
9. Ryakhovskikh IV, Bogdanov RI, Ignatenko VE. Intergranular stress corrosion cracking of steel gas pipelines in weak alkaline soil electrolytes. Eng. Fail. Anal. 2018; 94: 87-95.
10. Bin H, Pengju H, Lifeng H, et al. Understanding the effect of soil particle size on corrosion behavior of natural gas pipeline via modelling and corrosion micromorphology. Eng. Fail. Anal. 2017; 80: 325-340.
11. Asgari H, Toroghinejad MR, Golozar MA. Effect of coating thickness on modifying the texture and corrosion performance of hot-dip galvanized coatings. Curr. Appl. Phys. 2009; 9: 59-66.
12. AFNOR. NF X31-107, 2003.
13. ISO 10390, 2005.

14. R. Jean, Dunod 7e édition, pp. 220, 1984.
15. NF T 90-019, 1984.
16. NF EN 27888, 1994.
17. NF ISO 11464, 2006.
18. Flitt HJ, Schweinsberg DP. Synthesis, matching and deconstruction of polarization curves for the active corrosion of zinc in aerated near-neutral NaCl solutions. Corros. Sci. 2010; 52: 1905-1914.
19. Mouanga M, Berçot P, Rauch JY. Comparison of corrosion behaviour of zinc in NaCl and in NaOH solutions. Part I: Corrosion layer characterization. Corros. Sci. 2010; 52: 3984-3992.
20. Muster TH, Cole IS. The protective nature of passivation films on zinc: surface charge. Corros. Sci. 2004; 46: 2319-2335.
21. Suedile F, Robert F, Roos C, et al. Corrosion inhibition of zinc by Mansoa alliacea plant extract in sodium chloride media: Extraction, Characterization and Electrochemical Studies. Electrochim. Acta. 2014; 133: 631-638.
22. Jones DA, Corr. Nace, vol. 28, pp. 421, 1972.
23. Trejo D, Monteiro PJ. Corrosion performance of conventional (ASTM A615) and low-alloy (ASTM A706) reinforcing bars embedded in concrete and exposed to chloride environments. Cem. Concr. Res. 2005; 35: 562-571.
24. da Costa Pereira RF, Dantas de Oliveira ES, Gomes de Andrade Lima MA, et al. Corrosion of Galvanized Steel Under Different Soil Moisture Contents. Brasilc, Mater. Res. 2015; 18: 563-568.